Identification of Nucleation Loci in Emulsion Polymerization Processes. I. New Information from Spectroscopy Studies

Vineet Shastry,[1] L. H. Garcia-Rubio[2]

[1]*Department of Chemical Engineering, University of South Florida, E. Fowler Avenue, Tampa, Florida 33620*
[2]*College of Marine Sciences, University of South Florida, 140 7th Avenue South, St. Petersburg, Florida 33701*

Received 28 May 2004; accepted 19 January 2005
DOI 10.1002/app.22054
Published online 9 February 2006 in Wiley InterScience (www.interscience.wiley.com).

ABSTRACT Particle nucleation is the forcing function in emulsion polymerization reactions and as such it plays a significant role in the development of most of the properties of the final latex. The locus of nucleation in emulsion polymerization remains a contentious issue. Recent developments in the spectroscopy of emulsions strongly suggest that the locus of particle nucleation is a population of small nano-droplets of size range between 30–100 nanometers in diameter. These nano-droplets are generated independently of the rate of initiator decomposition and appear to be functions only of the emulsification conditions. In this paper the simulation studies leading to the identification of the nano-droplet population are described. The theoretical evidence suggesting that the nano-droplets are the main loci of particle nucleation is presented and along with the recommendations for the experimental work. © 2006 Wiley Periodicals, Inc. J Appl Polym Sci 100: 2847–2857, 2006

Key words: emulsion polymerization; particle nucleation; UV-vis spectroscopy

INTRODUCTION

Emulsion polymerization is a process of considerable industrial importance used in the manufacture of a wide range of products including paints, toners, adhesives, coatings, and other synthetic materials. It has applications in bioseparations through the functionalization of latex particles and offers great promise for the synthesis of nanomaterials. Particle nucleation is the forcing function in emulsion polymerization processes, and as such, it plays a significant role in the development of most of the properties of the final latex.[1] Particle nucleation is not fully understood and therefore remains an area of active research.[1,2] A complete understanding of the nucleation mechanism will ultimately enable the definition of optimal operating conditions to control the properties of the final latex.

The main locus for particle nucleation in emulsion polymerization is a subject of considerable controversy. Different theories advocate different loci.[1,2] Because the nucleation mechanism is highly influenced by the compositional and size characteristics of the actual nucleation sites, it is very important to identify and characterize them. This research effort primarily seeks to address the identification of the nucleation locus. The analysis and the results are reported in two parts.

A summary of accepted nucleation mechanisms and their limitations is presented in part I together with a new approach and the measurement techniques for the identification and characterization of the initial reaction conditions. Computer simulations and experimental data are also presented and discussed within the context of particle nucleation. In the backdrop of this discussion, a hypothesis for a likely nucleation locus is presented. This hypothesis is based on inferences drawn from simulation studies and from experimental observations that suggest the presence of a previously unidentified population of nanodroplets ranging in size from 30 to 100 nm. According to this study, the most likely locus for particle nucleation is this previously unidentified population of nanodroplets.

Part II focuses on the description and the reasoning behind the experimental efforts used to support the hypothesis proposed in part I. The effects of the initial emulsification conditions on the droplet populations are also reported in part II.

Definition of terms

To facilitate the presentation and discussion of this work, the following terms are defined:

Correspondence to: L. H. Garcia-Rubio (garcia@seas.marine.usf.edu).

Contract grant sponsor: Particle Engineering Research Center at the University of Florida; contract grant number: NSF EEC-94-02989.
Contract grant sponsor: ICI-Glidden.
Contract grant sponsor: Lucent Technologies.
Contract grant sponsor: Xerox.

© 2006 Wiley Periodicals, Inc.

Nanodroplets: Small droplets of the monomer ranging from 30 to 100 nm in diameter.
Time zero condition: Condition of the reaction mixture before the initiator is added (the beginning of the reaction). At time zero, the monomer is the dispersed oil phase in water, and this renders an oil-in-water emulsion.
Micelles: Aggregated molecules of surfactants, typically a few nanometers in diameter.
Swollen micelles: Micelles containing the monomer and ranging from 5 to 10 nm in diameter.[1]
Particle/polymer particles: Particles or droplets with either dead or growing polymer chains, ranging from 20 to 80 nm in diameter.[1]
Monomer droplets: Droplets of the monomer, ranging from 1 to 10 μm in size.[1]
Particle number: Number density of any particulate population: micelles, swollen micelles, polymer particles, monomer droplets, nanodroplets, and so forth.
Oligomeric radicals: Radicals containing three to five monomer units.
Forcing function: Cause of a particular response in a given process.

Proposed nucleation mechanisms

As previously indicated, there are several particle nucleation theories, each of which postulates different molecular or particulate entities as the main nucleation loci.[1–4] This section briefly discusses the accepted theories of particle nucleation in emulsion polymerization and their limitations. A detailed review can be found elsewhere.[5]

The particle nucleation theories proposed to date can be classified into three main groups depending on the locus for particle formation: micellar nucleation,[1–4] homogeneous nucleation, and coagulative nucleation. These theories have been formulated on the basis that the reaction mixture at time zero consists of micelles, monomer-swollen micelles, monomer droplets, and a continuous phase (water) containing the initiator and dissolved monomer.

Micellar nucleation mechanisms consider that the majority of particles are formed from the population of monomer-swollen surfactant micelles. The rate of particle nucleation is directly proportional to the micellar concentration and to the rate of capture of radicals by the micelles; which is function of the diffusivity of the oligomeric radicals.[1–4]

Hansen, Ugelstad, Fitch, and Tsai put forward a theory of homogeneous nucleation commonly called the HUFT theory.[1] In this case, the particles are initiated directly in the continuous phase from initiator radicals and dissolved monomer.

Coagulating events and the HUFT theory have been combined to form the homogeneous and coagulative nucleation theory,[1,6–9] which proposes that particle nucleation involves at least two mechanistic steps, as opposed to the single-step process required for micellar nucleation or for homogeneous nucleation. The first step is the formation of the precursor particles due to homogeneous nucleation. The second step is the formation of mature particles by the aggregation of the precursor particles. The rate of coagulation of the precursor particles is a function of their size and composition.[1]

The majority of the mechanisms proposed to date work in some instances and have suffered criticism for those cases in which the proposed models have been shown to be inadequate; for example; Gilbert[1] and Napper and Gilbert[6] discussed the limitations of the micellar nucleation theory, whereas Herrera Ordonez and Olayo[2] presented the limitations associated with the homogeneous and coagulative nucleation theory. In general, the main problem with all models published to date is that they contain many parameters relative to the observable (measurable) quantities accessible through the measurements, as indicated by Gilbert:[1] "with limited or inappropriate experimental data, one can readily find evidence in support of practically any mechanism".

Much of the difficulties encountered in obtaining information on nucleation mechanisms can be attributed to the lack of information on, or measurements of, variables that relate directly to the nucleation phenomena. In particular, experimental data on the initial distribution, composition, and number density of the particle populations present at the beginning of the reaction are not available. Furthermore, inferences on the nucleation mechanism from early-time particle size distribution (PSD) data are not reliable because the time constant for particle nucleation is much smaller than the time constant for sampling the PSD. For example, Giannetti[10] argued that most of the mechanistic information inferred from early-time PSD obtained from the experiments performed by Lichti et al.[2,10] is unreliable because of the stochastic broadening of the PSD that occurs after nucleation stops.

It is evident from the literature reports that knowledge of the PSD at the beginning, or at the early stages of the reaction, is critical for the identification of the nucleation loci and hence the nucleation mechanisms. Furthermore, it is also evident that, in addition to the measurement of the size distribution, reliable estimates of the particle counts must be obtained.

There are several techniques available for the characterization of the particle/droplet size distribution: Electron microscopy, angular laser light scattering, photon correlation spectroscopy, and dynamic light scattering are among the most widely used. Unfortunately, these techniques do not provide direct estimates of the particle counts, and in the case of electron microscopy, extensive sample preparations (i.e., vac-

uum evaporation) may be required, particularly when monomer-rich polymer particles are to be analyzed or when the dispersed phase has a high vapor pressure. Commercially available light scattering techniques are quite powerful and can be used directly for online applications. However, standard monochromatic light scattering techniques have difficulties resolving broad PSDs because the scattering contribution from large particles or droplets overwhelms the contribution to the total scattering from small particles when a mixed population of large and small particles is present.

Proposed approach

To identify the particle nucleation loci, in addition to an effective particle characterization technique, it is necessary to establish the state of the reacting mixture at the time of addition of the initiator (time zero). At this point, the reacting mixture is essentially a liquid–liquid emulsion. In contrast to previous studies,[1–4] in which inferences on the initial conditions were made on the basis of data sampled during early stages of the polymerization reactions, we propose to characterize the initial conditions of the reaction mixture through the study of liquid–liquid emulsions; ultraviolet–visible (UV–vis) spectroscopy techniques are ideally suited for this purpose and offer the following advantages:

1. Modern spectrometers are equipped with diode array technology, which enables the acquisition of the complete ultraviolet–visible–near-infrared (UV–vis–NIR) spectra with excellent wavelength resolution.[11–15]
2. The short measurement times of modern spectrometers enable real-time continuous monitoring applications.[15–20]
3. The resolution in terms of particle size near-infrared is proportional to the size parameter α ($\alpha = D/\lambda$, where D is the particle diameter and λ is the wavelength). Therefore, spectroscopy measurements over a broad range of wavelengths result in a large dynamic range for particle analysis. For example, if the complete UV–vis–NIR spectrum is acquired (190–1100 nm), populations of particles with sizes ranging from a few nanometers to a few micrometers can be simultaneously analyzed.[15–29]
4. In addition to the dynamic range for scattering, the absorption component, due to the presence of naturally occurring chromophores and/or labeled molecules, provides quantitative information for the estimation of the concentration of the chromophoric groups.[21–29]

As a first step in the study of the initial reaction conditions, preliminary spectroscopy data from emulsion polymerizations have been analyzed and compared with the theoretical simulations of their spectra.

SPECTROSCOPY INTERPRETATION MODEL

The equation that relates the transmission measured at a given wavelength λ_0 [$\tau(\lambda_0)$] and the normalized PSD for homogeneous particles [$f(D)$] is well known:[30]

$$\tau(\lambda_0) = N_p \lambda \left(\frac{\pi}{4}\right) \int_0^\infty Q_{\text{ext}}[m(\lambda_0),D] D^2 f(D) dD \quad (1)$$

where ℓ is the path length, Q_{ext} corresponds to the Mie extinction efficiency, and N_p is the number of particles per unit of volume. The total extinction efficiency $\{Q_{\text{ext}}[m(\lambda_0),D]\}$ is a function of the optical properties of the particles and suspending medium through the complex refractive index [$m(\lambda_0)$]:[31]

$$m(\lambda_0) = \frac{n(\lambda_0) + i\kappa(\lambda_0)}{n_0(\lambda_0)} \quad (2)$$

where $n(\lambda_0)$ and $\kappa(\lambda_0)$ represent the real and imaginary components of the complex refractive index of the particles, respectively, and $n_0(\lambda_0)$ represents the real refractive index of the suspending medium.

Under the assumption that the fundamental scattering model described in eqs. (1) and (2) applies to mixtures of particles, it is proposed to approximate the complex reacting mixture present in emulsion polymerizations by the consideration of M groups or populations,[32] each of which will be characterized by its corresponding scattering and absorption components. The characteristic dimensions of a population with its corresponding optical properties will largely define the scattering contribution to the observed spectrum, whereas the absorption contribution will be defined by the chemical composition of the population, in particular by its chromophoric content. For example, the following groups may be considered distinct populations: the monomer-swollen polymer particles, monomer droplets, micelles, free emulsifier, and so forth. The total scattering and absorption components of the spectrum will be given by the weighted sum of the contributions from the M populations. With this approach, it is possible to formulate and test hypotheses concerning the location and properties of the chromophoric groups and the scattering elements contained in the reacting mixture.

Under these approximations, the turbidity spectrum of an emulsion can be written in terms of M distinct populations:[32]

$$\tau(\lambda_0) = N_p \lambda \left(\frac{\pi}{4}\right) \sum_{i=1}^{M} x_i \int_0^\infty Q_{\text{ext}i}[m_i(\lambda_0),D] D^2 f_i(D) dD \quad (3)$$

where m_i is the complex refractive index and x_i ($i = 1 \rightarrow M$) is the number fraction corresponding to each population such that

$$\sum_{i=1}^{M} x_i = 1 \tag{4}$$

The real and imaginary parts of the complex refractive index are functions of the chemical composition and can be calculated as a weighted sum of the contributions from the chromophores within each population:

$$n_i = \sum_{j=1}^{N_i} \omega_{ij} n_{ij} \tag{5}$$

$$k_i = \sum_{j=1}^{N_i} \omega_{ij} k_{ij} \omega \tag{6}$$

where ω_{ij} represents the mass fraction of the jth chromophore contained in the ith population; n_i and k_i correspond to the real and imaginary refractive indices of each population, respectively; and N_i represents the total number of chromophoric groups in the ith population. Assuming volume additivity, the total concentration (c_{total}) of any chromophoric group can be readily calculated in terms of the concentration of each population (c_i):

$$c_{\text{total}} = \sum_{i=1}^{M} c_i \tag{7}$$

The additivity of the optical properties applies only within each population. Adding the scattering contributions represented by eqs. (3)–(6) closes the total mass balance for each chromophoric group.

EXPERIMENTAL

Materials

Styrene monomer was obtained from Aldrich Chemical Co. (St. Louis, MO). The surfactant sodium lauryl sulfate and the initiator potassium persulfate were obtained from Sigma Chemical Co. (St. Louis, MO) Sodium bicarbonate, used as a buffer for maintaining the pH of the reaction mixture, was obtained from J. T. Baker Chemical Co. (NJ).

For the experiments with decane–water–sodium dodecyl benzene sulfonate (SDBS) emulsion systems, decane and SDBS were from Sigma–Aldrich (St. Louis, MO).

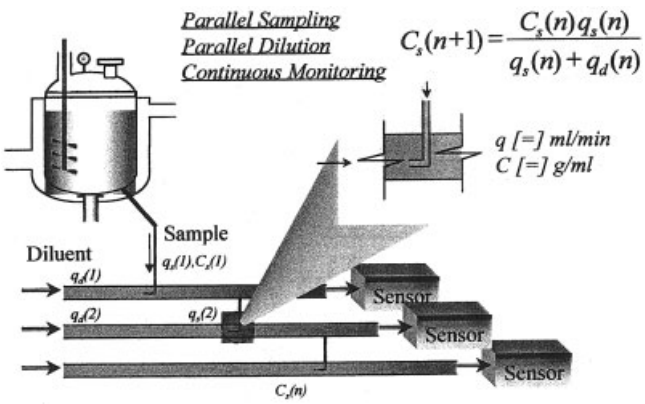

Figure 1 Schematic of the automatic sampling and dilution system used for online continuous monitoring of emulsion polymerizations and liquid–liquid emulsions (see refs. 18, 19, and 26).

Reactor and sampling system

Successful sampling of liquid–liquid emulsions and emulsion polymerization reactions, in terms of representative sampling and sample integrity, can be accomplished with the reactor configuration and the automatic sampling and dilution system described by Sacoto and coworkers.[18,19] Figure 1 shows the schematic of the reactor and the dilution system that enables real-time continuous spectroscopy measurements of the reacting mixture.

Spectroscopy measurements

Online and offline transmission UV–vis spectra were recorded with a diode array spectrometer (HP 8452-A, Hewlett–Packard, Palo Alto, CA) with an acceptance angle lower than 2°. All measurements, unless otherwise indicated, were conducted at room temperature with a 1-cm-path-length cuvette.

Normalization of the spectra

To eliminate concentration and particle number effects, both the measured and calculated transmission spectra were normalized with the integral of the optical density evaluated between 230 and 820 nm:[32]

$$\tau(\lambda) = \left(\frac{\tau_0(\lambda)}{\int_{\lambda_i}^{\lambda_f} \tau_0(\lambda) d\lambda} \right) \tag{8}$$

where λ_i and λ_f are the initial and final wavelengths, respectively, selected for normalization. This step enables the direct comparison of the spectral features without an independent estimation of the number of particles.

TABLE I
Emulsion Polymerization Recipe

Nano pure distilled water	662 g
Styrene	228 g
Sodium lauryl sulfate	10 g
Sodium bicarbonate	1.0 g
Potassium persulfate	1.0 g
Temperature	60°C
rpm	300

Optical properties

The optical properties of the continuous phase [refractive index $n_0(\lambda_0)$] under the reaction conditions were estimated with the expression developed by Scheibener.[33] These values are in good agreement with the values reported by Celis.[34] The optical properties of styrene monomer were approximated from its measured solution spectrum and the Kramer–Kronigs transforms.[30,31] The optical properties of decane at different temperatures were estimated with the Sellimeir–Drude equation.[34] The procedures for calculating the optical properties of the continuous phase and decane are detailed elsewhere.[5]

Scattering calculations

The Mie scattering efficiencies in eq. (3) were evaluated with a computer program that includes multiwavelength spectral calculations and has been adapted to calculate distributions of particle sizes.[15] This program has been extensively tested against available computer codes and published tables.[15]

Emulsion polymerizations

The monomer-in-water emulsions were prepared according to the recipe given in Table I. In a 1-L jacketed reactor, 662 mL of water was initially added to the reactor and was followed by the buffer, sodium bicarbonate, and the surfactant, sodium lauryl sulfate. Styrene monomer was then added to the contents of the reactor. The contents of the reactor were emulsified at 60°C and 300 rpm. After emulsification, the polymerization reaction was started with the addition of the initiator, potassium persulfate. The reaction was run in an inert atmosphere of argon. A sample slip stream of the emulsion was continuously drawn from the reactor and pumped into the dilution system to bring the concentration of the reacting mixture within the linear range of the spectrometer.[18,19] The reacting mixture was then continuously monitored. At the desired sampling intervals, the spectra were stored for further analysis.

RESULTS

Figure 2 shows a typical normalized transmission spectrum of the styrene-in-water emulsions before the addition of the initiator (time zero). Note that the ordinate corresponds to the normalized optical density. As indicated previously, the measured optical density was normalized with eq. (6) to eliminate the effect of the particle concentration.[32] After normalization, the observed spectral features are functions only of the size distribution of the droplet populations present in the emulsion.[32] The experimentally measured spectra show two distinct regions: a scattering-dominated region at longer wavelengths (300–820 nm) that reflects a broad droplet size

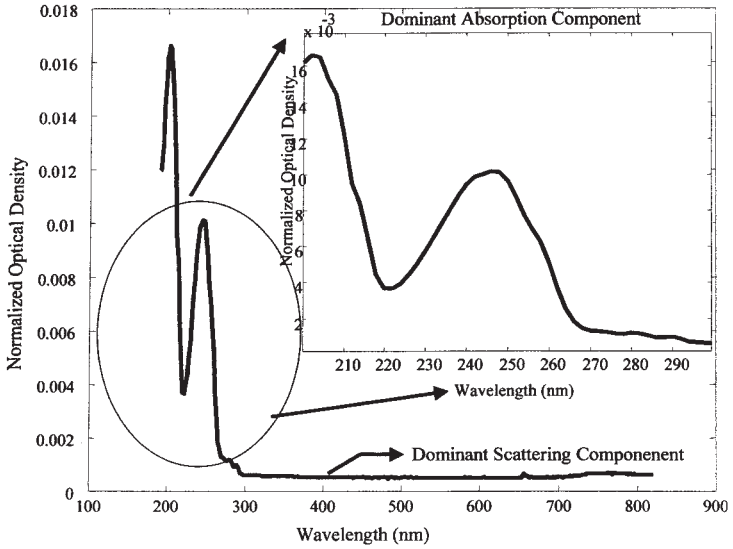

Figure 2 Normalized transmission spectrum of a typical styrene-in-water emulsion before the addition of the initiator (time zero condition).

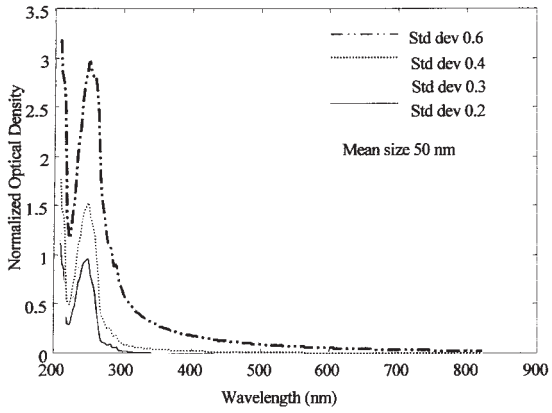

Figure 3 Predicted changes in the shape of transmission spectra of styrene-in-water emulsions as functions of the standard deviation of the droplet size distribution and the constant mean diameter.

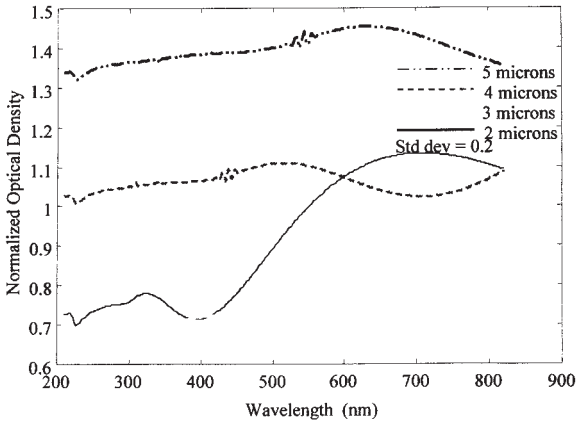

Figure 5 Predicted changes in the shape of transmission spectra of large droplets of styrene-in-water emulsions as functions of the mean droplet diameter and the constant standard deviation of the size distribution.

distribution and an absorption-dominated region at shorter wavelengths (190–300 nm) in which the absorption due to the phenyl moiety and the double bond of the styrene monomer are known to be present. The portion of the spectrum in which styrene absorption dominates is shown in the insert (Fig. 2). The spectral features of the absorption component of the experimental spectrum do not reflect pure styrene monomer absorption; instead, these features closely resemble those present in the simulated spectra of small-droplet populations (Fig. 3).

SSNSITIVITY ANALYSIS

With eqs. (3)–(7), it is possible to investigate the expected spectral response of individual components known to be present in the emulsion polymerization reacting mixtures and to assess the relative contribution of each component and/or population to the total spectra. Figures 3–6 depict the changes in the simulated transmission UV–vis spectrum of a hypothetical two-component styrene-monomer-in-water emulsion. Considerable changes are reflected in the shape of the simulated spectrum as a result of changes in the mean diameter and standard deviation of the droplet populations. Also, the mean droplet sizes correspond to populations known to be present in emulsion polymerizations.[1] Figures 3 and 4 illustrate the three main features of the transmission spectra when both absorption and scattering are present. Styrene monomer is a strong chromophore, with the main absorption bands due to the phenyl group and the vinyl double bond appearing between 200 and 300 nm. For small particle sizes, the absorption component dominates, and the absorption bands due to the monomer are clearly discernable. The spectral region between 300 and 820 nm reflects primarily the scattering effects; therefore, as the size of the particles increases, there is a concomitant increase in extinction. As the particle size increases and scattering dominates over absorp-

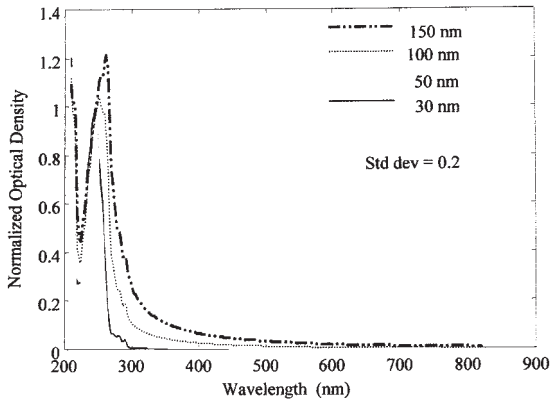

Figure 4 Predicted changes in the shape of transmission spectra of styrene-in-water emulsions as functions of the mean droplet diameter and the constant standard deviation of the size distribution.

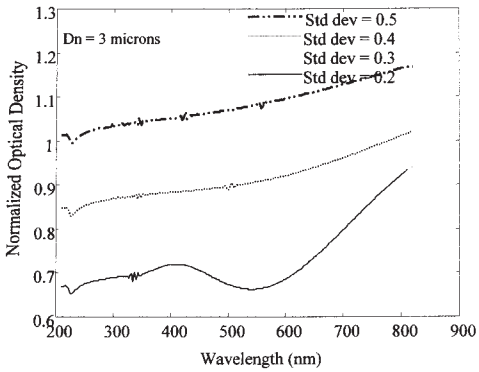

Figure 6 Predicted changes in the shape of transmission spectra of large droplets of styrene-in-water emulsions as functions of the standard deviation of the droplet size distribution and the constant mean droplet diameter (D_n).

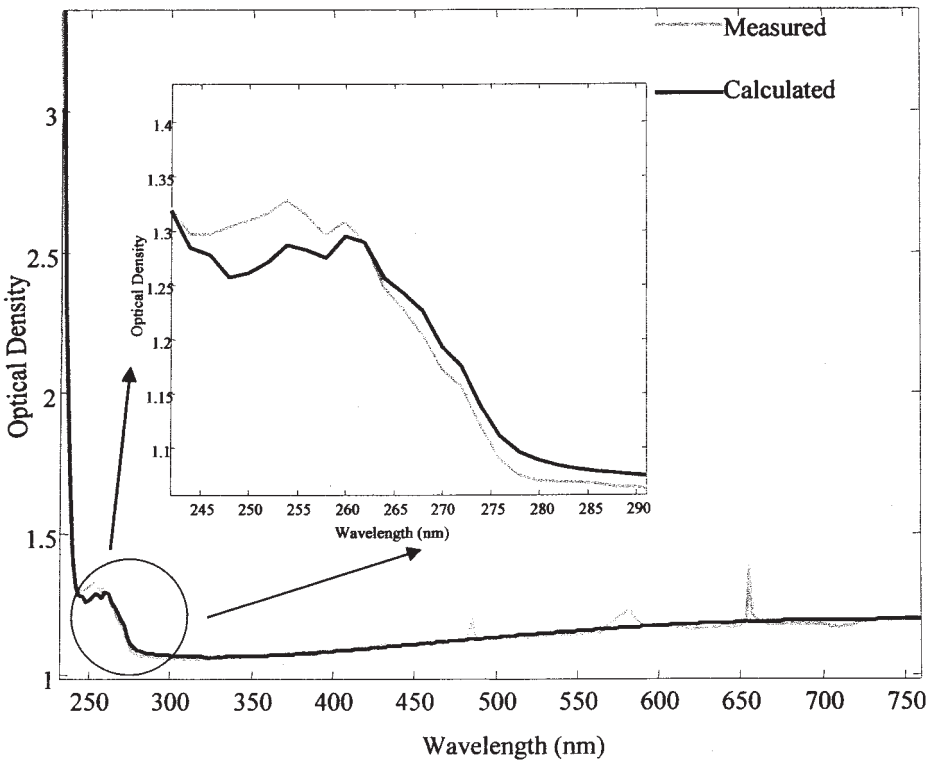

Figure 7 Comparison of the measured and calculated spectra of a decane-in-water emulsion with SDBS as the emulsifier.[34] The spectral features due to the emulsifier can be observed in the wavelength region of 240–280 nm.

tion, the features of the absorption bands decrease until, as shown in Figures 5 and 6, the absorption bands practically disappear. It is also apparent from Figures 3–6 that as the breath of the size distribution increases, the spectral features become smoother. This is due to the averaging of the spectral features. An important observation can be made at this point in reference to the experimentally measured spectra (Fig. 2). If the styrene monomer were present only in large droplets, the spectral features due to absorption would not be discernible. The fact that there is absorption suggests that the monomer is either in solution or contained in small particles. Furthermore, because the measured absorption features do not correspond to pure monomer absorption, the experimental data suggest that the monomer may be partitioned between monomer droplets, monomer in solution, and a population of relatively small droplets (nanodroplets).

Because the presence of one or more droplet populations is directly related to the partitioning of the surfactant among the droplet populations, experimental measurements and simulations were conducted with a model emulsion system consisting of decane and SDBS as the surfactant. Decane was selected because it has physicochemical properties within the range of commercial monomers of interest and it does not have strong chromophoric groups that would overlap with the phenyl moiety of the surfactant (SDBS). Figure 7 shows a typical normalized UV–vis spectrum of a decane emulsion measured with the same system. Notice the absorption features between 200 and 300 nm, which are due to the phenyl moiety of the surfactant (SDBS), and the broad scattering features between 300 and 820 nm, which are due to the size distribution of the large-droplet population (5–10 μm).[5,34]

Extensive simulations and spectral deconvolution efforts have demonstrated that it is possible to ade-

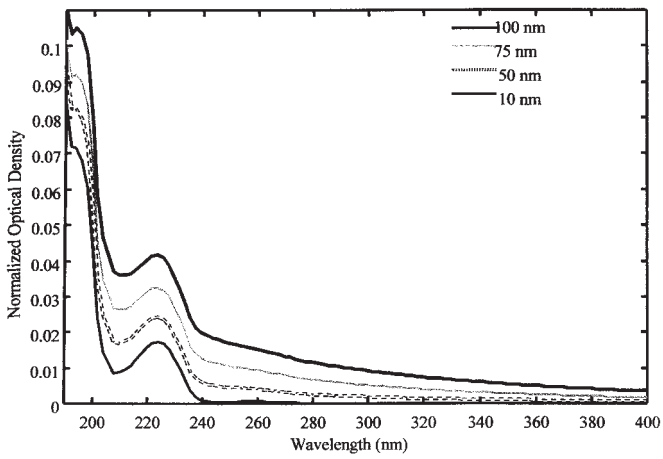

Figure 8 Comparison of the simulated transmission spectra of a decane-in-water emulsion (with SDBS as the emulsifier) for droplet populations of different sizes.

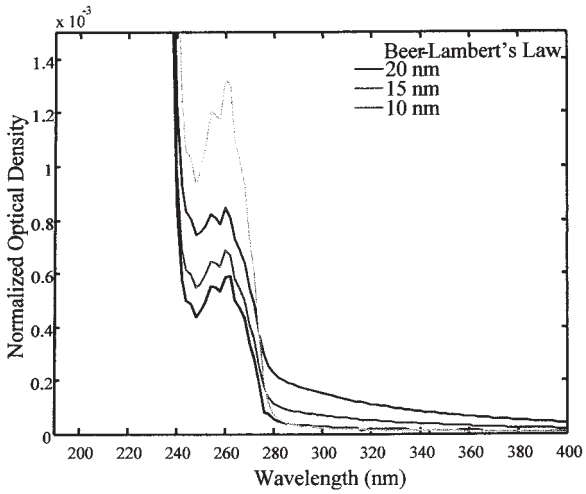

Figure 9 Effect of the droplet size on the simulated spectra of a decane-in-water emulsion consisting of small droplets (10–50 nm). Note the changes in the spectral features and amplitude as functions of the droplet size.

quately represent the spectral region between 300 and 820 nm with a broad droplet size distribution.[34,35] However, the broad droplet size distributions are unable to explain the spectral features between 200 and 300 nm, and this leads to two unresolved issues:

1. The presence of the strong absorption bands due to the emulsifier (Fig. 7) suggests that the emulsifier must be in solution, micelles, and/or small droplets (nanodroplets) because, as can be appreciated from Figures 4 and 8, the absorption features of the emulsifier essentially disappear for particle sizes greater than 50 nm.
2. The total concentrations of the oil phase, calculated on the basis of the broad droplet size distributions estimated from the spectral region between 300 and 820 nm, falls considerably short (50–20%) of the known concentration of the oil phase in the emulsion. This suggests that the identification of the droplet populations is incomplete.

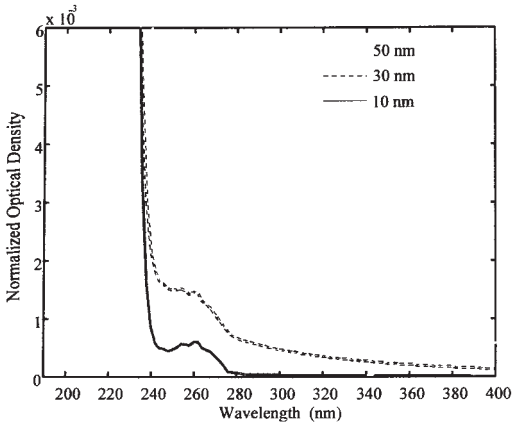

Figure 10 Comparison of the effect of the droplet size on the simulated transmission spectra of a decane-in-water emulsion (with SDBS as the emulsifier). Note the disappearance of the absorption features as the droplet size increases.

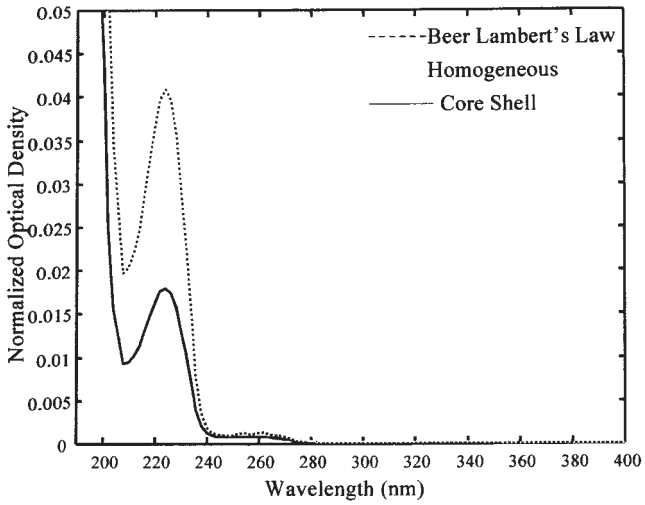

Figure 11 Comparison of the effect of the particle structure on the simulated transmission UV–vis spectra of a decane-in-water emulsion with SDBS as the emulsifier. The droplet size and the emulsifier/oil ratio are kept constant. Note the changes in the spectral features and amplitude of the emulsifier absorption bands (240–300 nm) as functions of the particle structure.

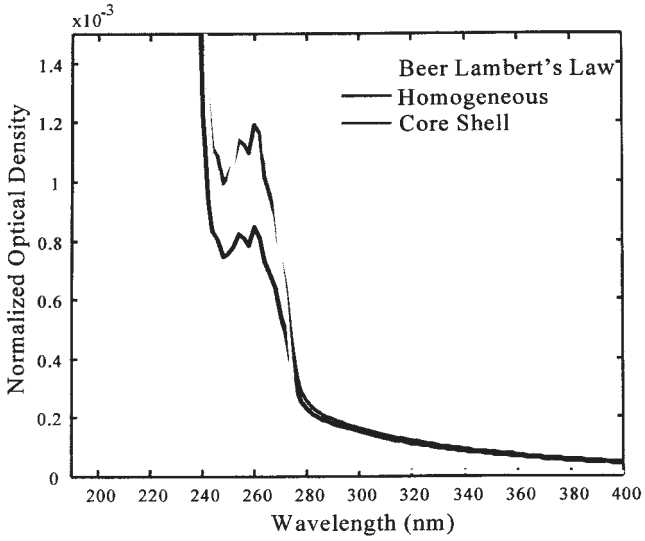

Figure 12 Comparison of the effect of the particle structure on the simulated transmission UV–vis spectra of a decane-in-water emulsion with SDBS as the emulsifier. The droplet size (30 nm) and the emulsifier/oil ratio are kept constant. Note the changes in the spectral features and amplitude of the emulsifier absorption bands (240–300 nm) as functions of the particle structure.

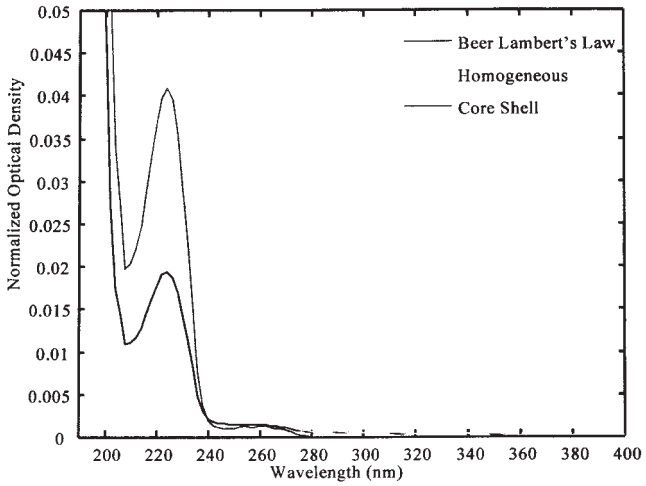

Figure 13 Comparison of the effect of the particle structure on the simulated transmission UV–vis spectra of a decane-in-water emulsion with SDBS as the emulsifier. The droplet size (30 nm) and the emulsifier/oil ratio are kept constant. Note the changes in the amplitude of the emulsifier main absorption bands at approximately 210 nm as a function of the particle structure.

To assist in the understanding how the oil phase may be distributed among different droplet populations and how these populations may reflect the observed spectral features, additional simulations aimed at exploring the effect of the droplet size, and the effect of the particle structure, on the spectra of *n*-decane/SDBS have been conducted. Figures 9–14 show the most important results. Figures 9 and 10 show the

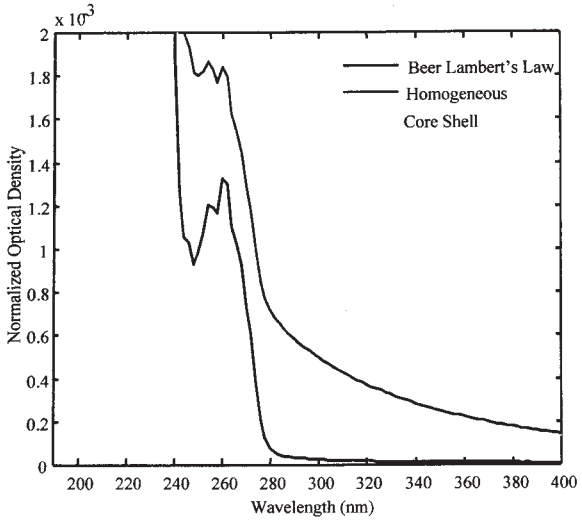

Figure 14 Comparison of the effect of the particle structure on the simulated transmission UV–vis spectra of a decane-in-water emulsion with SDBS as the emulsifier. The droplet size (50 nm) and the emulsifier/oil ratio are kept constant. Note the changes in the spectral features and amplitude of the emulsifier absorption bands (240–300 nm) as functions of the particle structure.

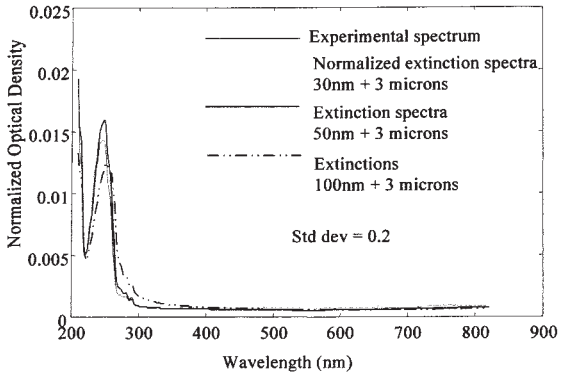

Figure 15 Comparison of the spectral features of the normalized experimental spectrum of a styrene-in-water emulsion with those of a simulated spectrum consisting of large and small droplets of different mean diameters added in equal proportions.

effect of the droplet size on the main absorption features of SDBS. As the size increases, the absorption band at approximately 220 nm persists, in a manner similar to the observations made for styrene monomer (Figs. 3 and 4). The effects of the droplet size on the absorption features due to the resonance structure of the phenyl moiety in SDBS (230–300 nm) are shown in Figures 8–10. As the droplet size increases, the absorption features decrease with respect to the contribution of the scattering component, and at approximately 50 nm, the absorption features almost disappear altogether. These results further suggest the presence of smaller particles (nanodroplets) in the emulsions, particularly when it is noticed that the scattering features arising from particles with sizes between 10 and 200

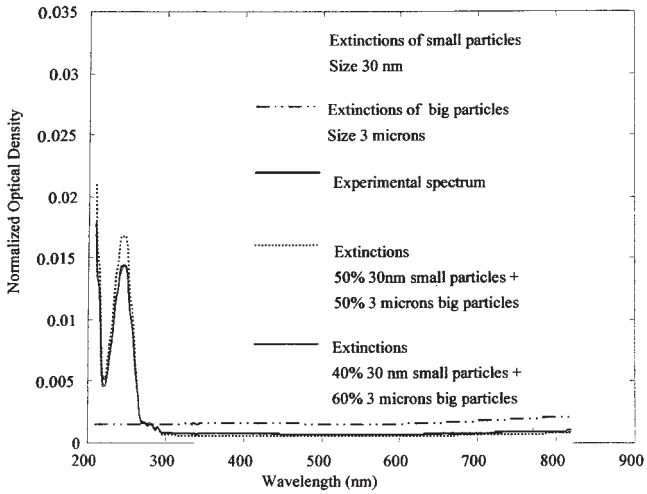

Figure 16 Comparison of the spectral features of the normalized experimental spectrum of a styrene-in-water emulsion with those of a simulated spectrum consisting of large (3 μm) and small (30 nm) droplets added in several proportions.

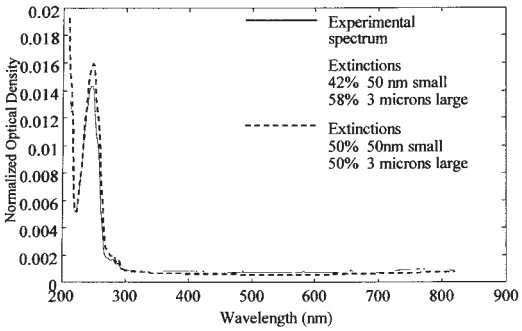

Figure 17 Comparison of the spectral features of the normalized experimental spectrum of a styrene-in-water emulsion with those of a simulated spectrum consisting of large (3 μm) and small (30 nm) droplets added in several proportions.

nm also appear in the spectral region between 200 and 400 nm.

The structure of the particles may also play a role in defining the spectral features of the emulsions.[5] Figures 11–14 show a comparison of the absorption and scattering behavior of the emulsifier (SDBS) in three different configurations: as a true solution (Beer–Lambert absorption), homogeneously distributed in the droplets, and as a layer in core–shell particles. For the simulations shown in Figure 12, the mass of emulsifier per unit of volume of emulsion was kept constant for the three configurations explored. A comparison of the spectra shown in Figure 12 with the measured spectra of decane emulsions (Fig. 7) clearly suggests that, in agreement with the experimental observations and with the simulations of styrene emulsions, most of the emulsifier must be associated with particles in the nanometer size range. Furthermore, the shape of the measured SDBS peaks (230–300 nm) also suggests that a core–shell structure would be the most appropriate model for the interpretation of this portion of the spectra.

Figures 15–17 have been used to further investigate the effects of mixed particle populations on the spectral features of styrene emulsions. Figures 15 and 16 show a comparison between typical measured spectra and simulated spectra. The simulated spectra in Figure 15 were calculated under the assumption of equal mass fractions of small particles of various sizes (30, 50, and 100 nm) and large-particle (3 μm) populations. Figure 16 shows the contribution of each particle population and the effect of varying the relative particle concentrations for the mixtures under consideration. Figure 17 shows that, by the consideration of two particle populations, nanodroplets and micrometer-size droplets, it is possible to obtain adequate representations of the measured spectra over a broad spectral range. An unexpected result from this analysis is the large mass fractions (~40%) of the oil phase required to be contained in the nanodroplet populations to match the measured spectra. It seems surprising that such large proportions of nanodroplets are required for the adequate representation of the spectra; however, there are two important elements supporting this conclusion: the closure of the mass balance of the oil phase and the consistency with the expectations from the theory of light scattering. The scattering per particle is much smaller for the nanoparticles than for the micrometer-size particles; therefore, a much larger number of the smaller particles will be required to yield comparable signals. In addition, the behavior of the absorption component supports not only the presence of nanodroplets but also the mass-balance conclusions.

CONCLUSIONS

The experimental data and the simulations reported herein clearly suggest that there are at least two distinct particle populations present in emulsion polymerization reacting mixtures before the addition of the initiator. These droplet populations can be readily identified from the measured spectra and consist of a previously unidentified population of nanodroplets with mean sizes between 30 and 100 nm together with a micrometer-size droplet distribution. The large mass fraction of the oil phase (40 to 50%) contained in the nanodroplet populations, with their concomitant large surface area, makes them likely loci for particle nucleation. It is also evident that the existence of a nanodroplet population does not preclude the presence of pure micelles and/or monomer-swollen micelles, which could also act as loci for particle nucleation. Similarly, the presence of a nanodroplet population does not preclude homogeneous nucleation or other competing nucleation mechanisms. What it does suggest is a different distribution of the emulsifier among the different particle populations present and a quantifiable element that may assist in bridging the particle nucleation theories proposed to date.

The identification of a well-defined nanodroplet population has considerable implications, not only in terms of particle nucleation but also in terms of the stability of emulsions and the distribution of emulsifiers. Therefore, we have undertaken a systematic study of liquid–liquid emulsions under conditions typical of emulsion polymerizations. The results of that study are reported in part II of this work.[5,36]

The authors acknowledge the Particle Engineering Research Center at the University of Florida and its industrial partners ICI-Glidden, Lucent Technologies, and Xerox for their financial and technical support. The authors also acknowledge Carl Biver for reviewing this article.

References

1. Gilbert, R. G. In Emulsion Polymerization: A Mechanistic Approach; Academic: San Diego, 1995.
2. Herrera-Ordonez, J.; Olayo, R. J Polym Sci A: Polym Chem 2000, 38, 2201.
3. Harkins, W. D. J Am Chem Soc 1947, 69, 1428.
4. El-Aasser, M. S.; Sudol, E. D. In Emulsion Polymerization and Emulsion Polymers; Lovell, P. A.; El-Aasser, M. S., Eds.; Wiley: Chichester, England, 1997; p 37.
5. Shastry, V. Ph.D. Dissertation, University of South Florida, 2004.
6. Napper, D. H.; Gilbert, R. G. In Comprehensive Polymer Science; Allen and Bevington: 1989; Part II, Chapter 4, p 171.
7. Feeney, P. J.; Napper; D. H.; Gilbert, R. G. Macromolecules 1984, 17, 2520.
8. Gilbert, R. G. In Emulsion Polymerization and Emulsion Polymers; Lovell, P. A.; El-Aasser, M. S., Eds.; Wiley: Chichester, England, 1997; p 165.
9. Feeney, P. J.; Napper, D. H.; Gilbert, R. J Colloid Interface Sci 1987, 118, 493.
10. Herrera-Ordonez, J.; Olayo, R. J Polym Sci Part A: Polym Chem 2000, 38, 2219.
11. The International Association for Properties of Waters and Steam (Release on Refractive Index of Ordinary Water Substance as a Function of Wavelength, Temperature and Pressure), http://www.protein-solutions.com/psi_books/light_scattering/dynamic/are_o_and_d_dc_temperature_dependent_.htm (accessed September 2003).
12. HP 8452 A Diode-Array Spectrophotometer Handbook; Hewlett–Packard: 1990.
13. OOIBase32 Spectrometer Operating Software Manual, version 1.0.; Ocean Optics: 2000.
14. Lambda Array 3840 UV/VIS Spectrophotometer Operating Directions (Preliminary); PerkinElmer: 1984.
15. Elicabe, G.; Garcia Rubio, L. H. Advances in Chemistry Series; American Chemical Society: Washington, DC, 1990; pp 83–104.
16. Brandolin, A.; Garcia-Rubio, L. H.; Provder, T.; Koehler, M. E.; Kuo, C. ACS Symposium Series; American Chemical Society: Washington, DC, 1991; pp 20–33.
17. Vara, J. Master's Thesis, University of South Florida, 2000.
18. Sacoto, P.; Lanza, F.; Suarez, H.; Garcia-Rubio, L. H. In Particle Size Distribution III: Assessment and Characterization; Provder, T., Ed.; ACS: Washington, DC, 1996; p 23.
19. Sacoto, P. J. M.S. Thesis, University of South Florida, 1999.
20. Mattley, Y. Ph.D. Dissertation, University of South Florida, 2000.
21. Imeokparia, D. Ph.D. Dissertation, University of South Florida, 1991.
22. Shetty, S. Ph.D. Dissertation, University of South Florida, 1993.
23. Throckmorton, J. L. Ph.D. Dissertation, University of South Florida, 1995.
24. Bacon, C. P. Ph.D. Dissertation, University of South Florida, 1999.
25. Steimle, E. Ph.D. Dissertation, University of South Florida, 1999.
26. Cardenas, A. Ph.D. Dissertation, University of South Florida, 2001.
27. Fisher, S. M.S. Thesis, University of South Florida, 1998.
28. Thennadil, S. Ph.D. Dissertation, University of South Florida, 2001.
29. Mehta, J.; Garcia-Rubio, L. H. In Initiation Reaction and the Modeling of Polymerization Kinetics; Provder, T., Ed.; ACS Symposium Series 313; American Chemical Society: Washington, DC, 1986; p 202.
30. Kerker, M. The Scattering of Light and Other Electromagnetic Radiation; Pergamon: New York, 1969.
31. Bohren, C. F.; Huffman, D. R. Absorption and Scattering of Light by Small Particles; Wiley: New York, 1983; pp 29, 80, 81, and 135.
32. Alupoei, C. M.S. Thesis, University of South Florida, 2001.
33. Scheibener, P.; Straub, J.; Levelt-Sangers, J. M. H.; Gallagher, J. S. Phys Chem Ref data 1990, 19, 677.
34. Celis, M. Ph.D. Dissertation, University of South Florida, 2000.
35. Cardenas, A. M.; Shastry, V.; Garcia-Rubio, L. H. In *In Situ* Spectroscopy of Monomer and Polymer Synthesis; Puskas, J. E.; Long, T. E.; Storey, R. F., Eds.; Kluwer Academic/Plenum: New York, 2002; p 83.
36. Shastry, V.; Garcia-Rubio, L. H. J Appl Polym Sci 2005.